Macromolecules **2004,** *37,* 2353−2362

Synthesis of Polythiophene Derivatives Bearing Ferroelectric Liquid Crystalline Substituents

Hiromasa Goto,[†,‡] Xiaoman Dai,[‡] Harunori Narihiro,[‡] and Kazuo Akagi*,[†,‡,§]

Tsukuba Research Center for Interdisciplinary Materials Science (TIMS), Institute of Materials Science, and Center for Tsukuba Advanced Research Alliance (TARA), University of Tsukuba, Tsukuba, Ibaraki 305-8573, Japan

Received September 26, 2003; Revised Manuscript Received December 17, 2003

ABSTRACT: A chiral liquid crystalline (LC) substituent with a fluorine-containing asymmetric moiety was introduced into the 3-position of a thiophene ring. Polymerizations of 2,5-dibrominated thiophene derivatives were carried out through dehalogenative polycondensations. Polythiophene derivatives thus prepared were fusible and soluble in ordinary organic solvents. An absorption band was observed in the range of 400−415 nm. Phase transition behaviors of the polymers and monomers were examined by differential scanning calorimetry, polarizing optical microscopy, and X-ray diffraction analysis. The polymers showed several types of smectic phases in the heating and cooling processes. Additionally, one of the polymers exhibited a striated fan-shaped texture when observed with a polarizing optical microscope. This is attributed to the formation of chiral smectic C (SmC*) phase, which is necessary property to ferroelectricity. Ferroelectric behavior was confirmed by examining the temperature dependence of the dielectric constant of the polymer.

Introduction

Various types of liquid crystalline (LC) conjugated polymers have been successfully synthesized to cultivate fruitful molecular electronics.[1−7] Conjugated polymers with self-assembly properties can be obtained by substituting the backbone with mesogens or alkyl group to show liquid crystallinity.[8,9] The use of LC conjugated polymers is expected in electronic and optical devices due to the control of molecular order and macroscopic orientation. Namely, the control of the orientation of conjugated polymer main chains gives rise to the possibility of polarized electroluminescent devices.[10−16]

Polythiophene and its processable derivatives occupy an important position in the study of conjugated polymers. The polythiophenes have many attractive characteristics for application in polymer electroluminescence devices such as good electrical properties and stability.[11,12] Polythiophene derivatives with LC side chains are one of the most intriguing types of polymer[6] because their useful electrical and optical properties are expected to be controllable via the molecular orientation of LC side chain. Also, it is expected that the orientation of the LC side chain may enhance the main-chain coplanarity due to the spontaneous orientation of the LC group of the side chains. The main-chain orientation can be further improved and therefore result in improved electrical properties.

Molecular chirality of liquid crystals is an interesting subject, in particular the discovery of a number of new LC materials having ferroelectric phases (FLC), antiferroelectric phases (AFLC), and twist grain boundary phases (TGB). It is well-known that FLC molecules have the ability to respond more quickly to an electric field used as an external electric field than nonchiral LC ones and that the ferroelectric liquid crystallinity is due to spontaneous polarization generated in the chiral smectic C phase (SmC*) when it is surface stabilized.[18−22]

In this study we synthesized novel FLC polythiophene derivatives through introduction of a fluorine-containing chiroptical LC group into the 3-position of the thiophene ring, and we examined the temperature dependence of the dielectric constant in the framework of applications for electronic devices with high-speed response and with the aim of achieving higher structural order through ferroelectric liquid crystallinity.

Experimental Section

All experiments were performed under an argon atmosphere using Schlenk/vacuum line techniques. Tetrahydrofuran (THF), *N*,*N*-dimethylformamide (DMF), ethanol, acetone, and ether were distilled prior to use.

Proton nuclear magnetic resonance (^{1}H NMR) spectra were measured in $CDCl_3$ using a Bruker AM-500 FT-NMR spectrometer. Chemical shifts are represented in parts per million downfield from tetramethylsilane as an internal standard. Infrared spectra were measured with a JASCO FT-IR 550 spectrometer using the KBr method. Optical absorption spectra were measured at room temperature using a Hitachi U-2000 spectrometer with quartz cell. Phase transition temperatures were determined using a Perkin-Elmer differential scanning calorimeter (DSC 7) with a constant heating/cooling rate of 10 °C/min, and texture observations were made using a Nikon ECLIPS E 400 POL polarizing microscope equipped with a Linkam TM 600PM heating and cooling stage. Temperature calibration of the heating stage was carried out by using DSC.

The molecular weights of polymers were determined by gel permeation chromatography (GPC) using a Shodex A-80M column and a JASCO HPLC 870-UV detector with THF used as solvent during measurements, with the instrument calibrated by polystyrene standard. XRD measurements were performed with a Rigaku D-3F diffractometer, in which X-ray power and scanning rate were set at 1200 mW and 5 °C/min, respectively. The dielectric constant was measured by SOLARTRON 1260 impedance analyzer. A planar alignment type cell with a rubbed polyimide film on each of the ITO glass substrate, thickness of 4 μm (EHC Ltd.), was used for dielectric measurements.

[†] Tsukuba Research Center for Interdisciplinary Materials Science.

[‡] Institute of Materials Science.

[§] Center for Tsukuba Advanced Research Alliance.

* Corresponding author.

10.1021/ma0354492 CCC: $27.50

Scheme 1

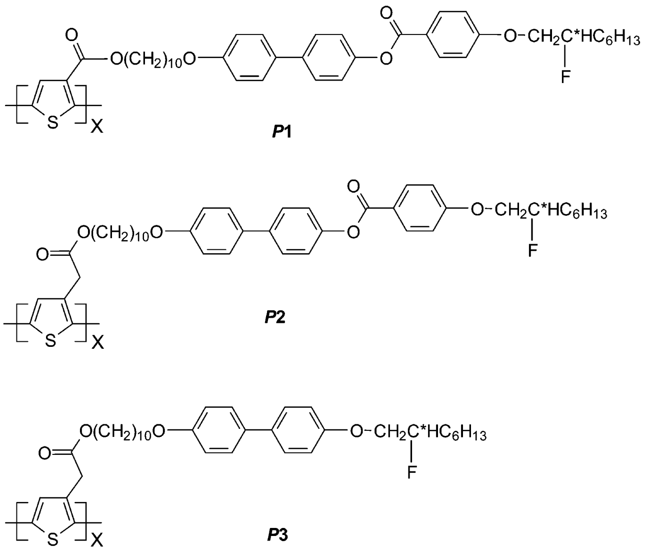

Three types of polythiophene derivatives containing fluorinated asymmetric moiety in the LC side chains were synthesized (Scheme 1). Characterizations of the polymers and corresponding monomers were carried out by means of differential scanning calorimetry (DSC), polarizing optical microscopy (POM), and X-ray diffraction (XRD). Molecular mechanics (MM) calculations were performed by a Silicon Graphics Cerius^2 system.

(*S*)-2-Fluorooctanol (1). To a stirred solution of pyridinium poly(hydrogen fluoride) (25 mL) in a Teflon flask was added dropwise via a syringe (*R*)-1,2-epoxyoctane (9.66 g, 75.5 mmol) in ether (37 mL) at 0 °C. The solution was stirred for 5 h under an argon atmosphere. Then the reaction mixture was poured into ~100 mL of crushed ice water. The crude product was extracted by ether and washed with water several times with a Teflon separating funnel. The organic layer was neutralized by saturated $\mathrm{NaHCO_3}$ solution and dried over anhydrous sodium sulfate. The solvent was removed by evaporation. Final purification by vacuum distillation yields 5.90 g (yield = 53.1%) of **1** as colorless liquid. $T_k = 68-72$ °C at 6 mmHg. IR (cm^{-1}): 3399, 2929, 2859, 1466, 1378, 1062, 843, 725. ^{1}H NMR ($\mathrm{CDCl_3}$, δ from TMS, ppm): 0.89 (t, 3H, J = 6.9 Hz, $-\mathrm{CH_3}$), 1.29−1.72 (m, 10H, $-\mathrm{CH_2CHF}(CH_2)_5\mathrm{CH_3}$), 2.56 (s, 1H, $-\mathrm{CHFCH_2}OH$), 3.60−3.73 (m, 2H, $-\mathrm{CHF}CH_2\mathrm{OH}$), 4.49−4.63 (dm, 1H, $-\mathrm{OCH_2}CHF-$).

Ethyl 4-[(*S*)-2-Fluorooctoxy]benzoate (2). To a solution of triphenylphosphine (9.44 g, 36 mmol) and ethyl *p*-hydroxybenzoate (6.0 g, 36 mmol) in THF (80 mL), a mixture consisting of diethyl azodicarboxylate, DEAD (16.0 g, 40 wt % in toluene, 36 mmol), and (*S*)-2-fluorooctanol (4.44 g, 30 mmol) in THF (90 mL) was very slowly added via pressure equalized dropping funnel. The reaction mixture was stirred at room temperature overnight under an argon atmosphere. TLC indicated completion of the reaction. The precipitate was filtered, the filtrate was evaporated to remove the solvent, and the residue was purified by column chromatography (silica gel, hexane/ethyl acetate = 2/1). The product was recrystallized from *n*-hexane: ethyl acetate and dried under vacuum to give 8.01 g of **2** as colorless crystal. Yield = 53 %; mp = 47−48 °C. IR (cm^{-1}): 2931, 2856, 1734, 1607, 1513, 1250, 1194. ^{1}H NMR ($\mathrm{CDCl_3}$, δ from TMS, ppm): 0.89 (t, 3H, J = 6.8 Hz, $-CH_3$), 1.19−1.86 (m, 13H, $-\mathrm{OCH_2}\boldsymbol{CH_3}$, $-\mathrm{CH_2CHF}(\boldsymbol{CH_2})_5\mathrm{CH_3}$), 4.04−4.13 (m, 2H, $-\mathrm{PhO}CH_2\mathrm{CHF}-$), 4.34 (q, 2H, J = 7.1 Hz, $-\mathrm{COO}CH_2\mathrm{CH_3}$), 4.75−4.88 (dm, 1H, $-\mathrm{OCH_2}CHF-$), 6.93 (d, 2ArH, J = 8.9 Hz, *ortho* to $-\mathrm{OCH_2CHF}-$), 7.99 (d, 2ArH, J = 8.9 Hz, *meta* to $-\mathrm{OCH_2CHF}-$).

4-[(*S*)-2-Fluorooctoxy]benzonic Acid (3). Compound **2** was hydrolyzed by potassium hydroxide (2.69 g, 40.0 mmol) in 15 mL of water and 24 mL of methanol at 50 °C for 4 h under an argon atmosphere. TLC indicated completion of the reaction. Then the solvent was evaporated, and it was dissolved in water. The mixture was acidified to pH = 2 by hydrochloric acid solution. The resulting precipitate was extracted with ether, thoroughly washed with water, and dried over anhydrous $\mathrm{MgSO_4}$. The ether was removed by evaporation and dried under reduced pressure to yield 3.55 g of **3**. Yield = 98.1 %. IR (cm^{-1}): 2930, 2859,1686, 1604, 1514, 1258, 1172. ^{1}H NMR ($\mathrm{CDCl_3}$, δ from TMS, ppm): 0.90 (t, 3H, J = 6.9 Hz, $-CH_3$), 1.25−1.86 (m, 10H, $-\mathrm{CH_2CHF}(CH_2)_5\mathrm{CH_3}$), 4.08−4.17 (m, 2H, $-\mathrm{PhO}CH_2\mathrm{CHF}-$) 4.34 (q, 2H, J = 7.1 Hz, $-\mathrm{COO}CH_2\mathrm{CH_3}$), 4.78−4.91 (dm, 1H, $-\mathrm{OCH_2}CHF$), 6.97 (d, 2ArH, J = 8.9 Hz, *ortho* to $-\mathrm{OCH_2CHF}-$), 8.07 (d, 2ArH, J = 8.9 Hz, *meta* to $-\mathrm{OCH_2CHF}-$).

1-Bromo-10-(2-tetrahydropyranyloxy)decane (4). A catalytic amount of pyridinium *p*-toluenesulfonate (PPTS) (~250 mg, 1 mmol) was added to a solution of 10-bromodecanol (10.0 g, 42 mmol) and 3,4-dihydro-2*H*-pyrane (DHP) (5.5 g, 63 mmol) in $\mathrm{CH_2Cl_2}$ (120 mL). The mixture was stirred under reflux for 3 h under an argon atmosphere. TLC indicated completion of the reaction. The reaction mixture was allowed to warm to room temperature and was washed with water twice and dried over anhydrous $\mathrm{MgSO_4}$. The solvent was evaporated, and the crude product was purified by column chromatography (silica gel, *n*-hexane/ethyl acetate = 20/1) to give 12.47 g of **4**. Yield = 92.4 %. IR (cm^{-1}): 2928, 2854, 1464, 1120, 1078. ^{1}H NMR ($\mathrm{CDCl_3}$, δ from TMS, ppm): 1.26−1.86 (m, 22H, cyclic, $-\mathrm{OCH_2}(\boldsymbol{CH_2})_3$; $-\mathrm{OCH_2}(CH_2)_8\mathrm{CH_2Br}$) 3.34−3.52 (dm, 2H, $-\mathrm{O}CH_2(\mathrm{CH_2})_8\mathrm{CH_2Br}$) 3.40 (t, 2H, J = 6.8 Hz, $-CH_2\mathrm{Br}$) 3.71−3.89 (dm, 2H, cyclic $-\mathrm{O}CH_2(\mathrm{CH_2})_3$) 4.57 (dd, 1H, J = 4.4 Hz, cyclic, $-\mathrm{O}CH$ $\mathrm{OCH_2}-$).

4-Hydroxy-4′-(10-(2-tetrahydropyranyloxy)decanyloxy)-biphenyl (5). Compound **4** (10.0 g, 31 mmol) in *n*-butanol (50 mL) was added dropwise to a suspension of 4,4′-biphenyldiol (17.0 g, 91 mmol) and anhydrous potassium carbonate (10.0 g, 91 mmol) in *n*-butanol (200 mL) at 80 °C. The reaction mixture was heated under reflux for 24 h under an argon atmosphere. TLC indicated completion of the reaction. The potassium bromide precipitate and excess potassium carbonate were filtered off, and the filtrate was evaporated. The solid was poured into large amount of $\mathrm{CH_2Cl_2}$ and filtered to remove the excess 4,4′-biphenyldiol, and the solvent was evaporated. Purification of the product was carried out by column chromatography (silica gel, hexane/ethyl acetate = 2/1) to give a white solid. Recrystallization from ethanol afforded 9.93 g of **5** as white crystal (yield = 75.2 %). IR (cm^{-1}): 3350, 2931, 2917, 2852, 1610, 1502, 1250, 1036, 821. ^{1}H NMR ($\mathrm{CDCl_3}$, δ from TMS, ppm): 1.21−2.04 (m, 22H, cylic $-\mathrm{OCH_2}(CH_2)_3$; $-\mathrm{OCH_2}(CH_2)_8\mathrm{CH_2O}-$), 3.36−3.52 (dm, 2H, $-\mathrm{O}CH_2(\mathrm{CH_2})_9\mathrm{OPh}-$), 3.71−3.90 (dm, 2H, cylic $-\mathrm{O}CH_2(\mathrm{CH_2})_3$), 3.98 (t, 2H, J = 6.6 Hz, $-\mathrm{PhO}CH_2(\mathrm{CH_2})_9\mathrm{O}-$), 4.58 (dd, 1H, J = 4.4 Hz, cylic, $-\mathrm{O}CH$ $\mathrm{OCH_2}-$), 4.71 (s, 1H, $-\mathrm{O}H$), 6.87 (d, 2ArH, J = 8.6 Hz, *ortho* to $-\mathrm{OH}$), 6.94 (d, 2ArH, J = 8.7 Hz, *ortho* to $-\mathrm{OCH_2}-$), 7.42 (d, 2ArH, J = 8.6 Hz, *meta* to $-\mathrm{OH}$), 7.44 (d, 2ArH, J = 8.7 Hz, *meta* to $-\mathrm{OCH_2}-$).

4-(4′-(10-(2-Tetrahydropyranyloxy)decanyloxy))-biphenyl-4-(2-fluorooctanyloxy)benzoate (6). Compound **3** (2.0 g, 7.5 mmol) was added to a solution consisting of **5** (4.8 g, 11.2 mmol), [4-(dimethylamino)pyridine] (DMAP) (1.37 g, 11.2 mmol), and (*N,N*′-dicyclohexylcarbodiimade) (DCC) (2.31 g, 11.2 mmol) in 100 mL of absolute dichloromethane. The solution was stirred for 24 h at room temperature under an argon atmosphere, TLC indicated completion of the reaction. Then the reaction mixture was filtered and filtrate was evaporated. The residue was purified with column chromatography (silica gel; hexane/ethyl acetate = 2/1), followed by recrystallization with ethanol to give 4.38 g of **6** as white solid. Yield = 86.4 %. IR (cm^{-1}): 2938, 2858, 1733, 1607, 1498, 1263, 1217, 1170, 1079, 1037, 843, 801. ^{1}H NMR ($\mathrm{CDCl_3}$, δ from TMS, ppm): 0.91 (t, 3H, J = 6.8 Hz, $-CH_3$), 1.21−2.17 (m, 32H, cylic $-\mathrm{OCH_2}(CH_2)_3$; $-\mathrm{OCH_2}(CH_2)_8\mathrm{CH_2O}-$, $-\mathrm{OCH_2CHF}(CH_2)_5\mathrm{CH_3}$), 3.36−3.51 (dm, 2H, $-\mathrm{O}CH_2(\mathrm{CH_2})_9\mathrm{OPh}-$), 3.71−3.89 (dm, 2H, cylic $-\mathrm{O}CH_2(\mathrm{CH_2})_3$), 4.00 (t, 2H, J = 6.6 Hz, $-\mathrm{PhO}CH_2\mathrm{CH_2}-$), 4.11−4.20 (m, 2H, $-\mathrm{PhO}CH_2\mathrm{CHF}-$), 4.58 (dd, 1H, cylic $-\mathrm{O}CH$ $\mathrm{OCH_2}-$), 4.81−4.92 (dm, 1H, $-\mathrm{OCH_2}CHF-$), 6.97 (d, 2ArH, J = 8.5 Hz, *ortho* to $-\mathrm{OCH_2CH_2}-$), 7.01 (d, 2ArH, J = 8.7 Hz, *ortho* to $-\mathrm{OCH_2CHF}-$), 7.24 (d, 2ArH, *ortho* to

−OCO−), 7.51 (d, 2ArH, J = 8.5 Hz, *meta* to $-\mathrm{OCH_2CH_2}-$), 7.58 (d, 2ArH, J = 8.4 Hz, *meta* to −OCO−), 8.16 (d, 2ArH, J = 8.7 Hz, *meta* to −COO−).

4-(4′-(10-Hydroxydecanyloxy))biphenyl-4-(2-fluorooctanyloxy)benzoate (7). PPTS (80 mg) was added to a solution of compound **3** (4.00 g, 5.9 mmol) in 120 mL of ethanol and refluxed at 80 °C for 2 h under an argon atmosphere. TLC indicated completion of the reaction. After evaporation of the solvent, the residue was thoroughly washed with water and extracted with ether. The ether layer was dried over anhydrous $\mathrm{MgSO_4}$ overnight. The solution was evaporated and purified by column chromatography (silica gel, $\mathrm{CH_2Cl_2}$/acetone = 40/1) and recrystallized from ethanol to give 3.48 g (yield = 99.4%) of **7** as white solid.[1] IR ($\mathrm{cm^{-1}}$): 3323, 2927, 2853, 1727, 1607, 1498, 1258, 1221, 1086, 802. H NMR ($\mathrm{CDCl_3}$, δ from TMS, ppm): 0.90 (t, 3H, J = 6.9 Hz, $-\mathrm{CH_3}$), 1.19−1.88 (m, 26H, $-\mathrm{OCH_2CHF}(\mathit{CH}_2)_5\mathrm{CH_3}$; $-\mathrm{OCH_2}(\mathit{CH}_2)_8\mathrm{CH_2\ OH}$), 3.64 (t, 2H, J = 6.6 Hz, $-\mathrm{CH_2}\mathit{CH}_2\mathrm{OH}$), 4.00 (t, 2H, J = 6.5 Hz, $-\mathrm{PhO}\mathit{CH}_2\mathrm{CH_2}-$), 4.11−4.22 (m, 2H, $-\mathrm{PhO}\mathit{CH}_2\mathrm{CHF}-$), 4.80−4.94 (dm, 1H, $-\mathrm{OCH_2}\mathit{CHF}-$), 6.97 (d, 2ArH, J = 8.7 Hz, *ortho* to $-\mathrm{OCH_2CH_2}-$), 7.01 (d, 2ArH, J = 8.9 Hz, *ortho* to $-\mathrm{OCH_2CHF}-$), 7.25 (d, 2ArH, J = 8.7 Hz, *ortho* to −OCO−), 7.51 (d, 2ArH, J = 8.7 Hz, *meta* to $-\mathrm{OCH_2CH_2}-$), 7.58 (d, 2ArH, J = 8.5 Hz, *meta* to −OCO−), 8.18 (d, 2ArH, J = 8.8 Hz, *meta* to −COO−).

2,5-Dibromothiophene-3-carboxylic Acid (8). Thiophene-3-carboxylic acid (5 g, 39 mmol) was very slowly added to a solution of *N*-bromosuccinimide, NBS (15.1 g, 86 mmol), in 80 mL of DMF by a pressure-equalized dropping funnel. After the addition was complete, 10 mL of DMF was added to the reaction mixture, refluxed for 20 h at 50 °C under an argon atmosphere. The reaction vessel was wrapped with aluminum foil to shield the reaction from light. TLC indicated completion of the reaction. Then the reaction mixture was allowed to warm to room temperature. The solution was poured into large amount of saturated sodium sulfate cooled by ice water. The yellow precipitate was filtered off and recrystallized from an ethanol:water mixture to yield 7.98 g of **8** as white needlelike crystal. Yield = 71.2%. IR ($\mathrm{cm^{-1}}$): 3095, 2989, 2924, 2871, 2623, 2561, 2481, 1677, 1526, 1443, 1253, 1003, 905. ^{1}H NMR ($\mathrm{CDCl_3}$, δ from TMS, ppm): 7.43 (s, 1ArH, $\mathrm{BrC}\mathit{CH}\mathrm{C}-$), 13.34 (sb, 1H, $-\mathrm{COO}\mathit{H}$).

2,5-Dibromothiophene-3-acetic Acid (9). Thiophene-3-acetic acid (10 g, 70.3 mmol) was very slowly added to a solution of *N*-bromosuccinimide, NBS (30.2 g, 172 mmol), in 50 mL of DMF by a dropping funnel. After the addition, 10 mL of DMF was further added to the reaction mixture and refluxed at 50 °C for 20 h under an argon atmosphere. The reaction vessel was wrapped by aluminum foil to shield the reaction from light. TLC indicated completion of the reaction. Then the reaction mixture was allowed to warm to room temperature. The solution was poured into a large amount of saturated sodium sulfate cooled by ice water. The yellow precipitate was filtered off and recrystallized from an ethanol:water mixture to yield 13.2 g of **9** as white needlelike crystal. Yield = 63.0%. IR ($\mathrm{cm^{-1}}$): 3101, 2918, 1702, 1417, 1235, 1016, 829, 634, 474. ^{1}H NMR ($\mathrm{CDCl_3}$, δ from TMS, ppm): 3.63 (s, 2H, $\mathrm{CH_2}$), 6.95 (s, 1ArH, $\mathrm{BrC}\mathit{CH}\mathrm{C}$).

4-(10-(2-Tetrahydropyranyloxy))-4′-(2-fluorooctyloxy)biphenyl (10). A solution of **1** (467 mg, 3.1 mmol) and DEAD (1.60 g, 3.6 mmol, 40 wt % in toluene) in 7 mL of THF was added dropwise to a stirred mixture of **5** (1.28 g, 3.0 mmol) and TPP (944 mg, 3.6 mmol) in THF (5 mL). The resulting reaction mixture was stirred for a further 24 h under an argon atmosphere; TLC indicated completion of the reaction. The colored reaction mixture was then evaporated to remove solvent. The solid was washed with water thoroughly and extracted with ether. Then the organic layer was evaporated to remove solvent. Purification by column chromatography (silica gel, *n*-hexane/ethyl acetate = 2/1) afforded 0.732 g of **10** in 44.0% yield. IR ($\mathrm{cm^{-1}}$): 2932, 2854, 1608, 1503, 1275, 1252, 1037, 823, 807. ^{1}H NMR ($\mathrm{CDCl_3}$, δ from TMS, ppm): 0.93 (t, 3H, J = 6.9, $-\mathit{CH}_3$), 1.18−1.77 (m, 32H, cylic, $-\mathrm{OCH_2}(\mathit{CH}_2)_3$; $-\mathrm{OCH_2}(\mathit{CH}_2)_8\mathrm{CH_2O}-$; $-\mathrm{OCH_2CHF}(\mathit{CH}_2)_5\mathrm{CH_3}$), 3.29−3.45 (dm, 2H, $-\mathrm{O}\mathit{CH}_2\mathrm{CH_2}-$), 3.64−3.82 (dm, 2H, cylic, $-\mathrm{O}\mathit{CH}_2(\mathrm{CH_2})_3$), 3.91 (t, 2H, J = 6.6 Hz, $-\mathrm{PhO}\mathit{CH}_2\mathrm{CH_2}-$), 3.97−4.08 (m, 2H, $-\mathrm{PhO}\mathit{CH}_2\mathrm{CHF}-$), 4.58 (dd, 1H, J = 4.4 Hz, cylic, $-\mathrm{O}\mathit{CH}\mathrm{OCH_2}-$), 4.70−4.84 (dm, 1H, $-\mathrm{OCH_2}\mathit{CHF}-$), 6.87−6.89 (dd, 4ArH, J = 8.7, 8.8 Hz, *ortho* to $-\mathrm{OCH_2CHF}-$, *ortho* to $-\mathrm{OCH_2CH_2}-$), 7.38−7.40 (dd, 4ArH, J, 8.7 Hz, *meta* to $-\mathrm{OCH_2CHF}-$, *meta* to $-\mathrm{OCH_2CH_2}-$).

4-(2-Fluorooctanyloxy)-(4′-(10-hydroxydecanyloxy))biphenyl (11). A mixture of compound **10** (0.60 g, 1.2 mmol) and PPTS (15 mg) in ethanol was refluxed for 2 h at 80 °C under an argon atmosphere. TLC indicated completion of the reaction. Then the solvent was removed by evaporation. The crude product was washed with water thoroughly and extracted with ether. The organic layer was filtered and dried over anhydrous $\mathrm{MgSO_4}$ overnight. The solvent was evaporated, and purification by column chromatography (silica gel, $\mathrm{CH_2Cl_2}$/acetone = 40/1) followed by recrystallization from ethanol afforded 0.51 g of **10** in 99.8% yield. IR ($\mathrm{cm^{-1}}$): 3301, 2920, 2851, 1609, 1503, 1276, 1253, 1178, 1049, 824, 808. ^{1}H NMR ($\mathrm{CDCl_3}$, δ from TMS, ppm): 0.83 (t, 3H, J = 6.8, $-\mathit{CH}_3$), 1.16−1.80 (m, 26H, $-\mathrm{OCH_2}(\mathit{CH}_2)_8\mathrm{CH_2O}-$; $-\mathrm{CH_2CHF}(\mathit{CH}_2)_5\mathrm{CH_3}$), 3.29−3.45 (dm, 2H, $-\mathrm{O}\mathit{CH}_2\mathrm{CH_2}-$), 3.56 (q, 2H, J = 6.5 Hz, $-\mathit{CH}_2\mathrm{OH}$), 3.91 (t, 2H, J = 6.6 Hz, $-\mathrm{PhO}\mathit{CH}_2\mathrm{CH_2}-$), 3.97−4.08 (m, 2H, $-\mathrm{PhO}\mathit{CH}_2\mathrm{CHF}-$), 4.70−4.84 (dm, 1H, $-\mathrm{OCH_2}\mathit{CHF}-$), 6.87−6.90 (dd, 4ArH, J = 8.7 Hz, *ortho* to $-\mathrm{OCH_2CHF}-$, *ortho* to-$\mathrm{OCH_2CH_2}-$), 7.38−7.40 (dd, 4ArH, J = 8.6 Hz, *meta* to $-\mathrm{OCH_2CHF}-$, *meta* to $-\mathrm{OCH_2CH_2}-$).

10-(4-(4′-(4″-(2-Fluorooctyloxy)phenylcarbonyloxy))-biphenoxy)decyl 2,5-Dibromothiophene-3-carboxylate (M1). Compound **4 (**593 mg, 1.0 mmol) was added to a mixture of 2,5-dibromothiophene-3-carboxylic acid (**5**) (343 mg, 1.2 mmol), (dimethylamino)pyridine, DMAP 147 mg (1.2 mmol), and dicyclohexylcarbodiimide, DCC (246 mg, 1.2 mmol), in 15 mL of absolute $\mathrm{CH_2Cl_2}$ and further stirred for 24 h at room temperature under an argon atmosphere. TLC indicated completion of the reaction. Then the solution was filtered to remove the urea crystals, and the solvent was removed by evaporation. The crude product was purified by column chromatography (*n*-hexane/ethyl acetate = 2/1) and recrystallized from *n*-hexane/ethanol solution (= 2/1) to afford 904 mg of **M1** as colorless crystal. Yield > 99.9 %. IR ($\mathrm{cm^{-1}}$): 2925, 2852, 1716, 1605, 1498, 1215, 1171, 1086, 800, 763. ^{1}H NMR ($\mathrm{CDCl_3}$, δ from TMS, ppm): 0.91 (t, 3H, J = 6.9, $-\mathrm{CH_3}$), 1.21−1.89 (m, 26H, $-\mathrm{OCH_2CHF}(\mathit{CH}_2)_5\mathrm{CH_3}$; $-\mathrm{OCH_2}(\mathit{CH}_2)_8\mathrm{CH_2O}-$), 4.00 (t, 2H, J = 6.6 Hz, $-\mathrm{PhO}\mathit{CH}_2\mathrm{CH_2}-$), 4.09−4.22 (m, 2H, $-\mathrm{PhO}\mathit{CH}_2\mathrm{CHF}-$), 4.27 (t, 2H, J = 6.7 Hz, $-\mathrm{COO}\mathit{CH}_2\mathrm{CH_2}-$), 4.80−4.94 (dm, 1H, $-\mathrm{OCH_2}\mathit{CHF}-$), 6.97 (d, 2ArH, J = 8.7 Hz, *ortho* to $-\mathrm{OCH_2CH_2}-$), 7.01 (d, 2ArH, J = 8.9 Hz, *ortho* to $-\mathrm{OCH_2CHF}-$), 7.24 (d, 2ArH, J = 8.7 Hz, *ortho* to −OCO−), 7.35 (s, 1ArH, $-\mathrm{SBrC}\mathit{CH}\mathrm{C}-$), 7.51 (d, 2ArH, J = 8.7 Hz, *meta* to $-\mathrm{OCH_2CH_2}-$), 7.58 (d, 2ArH, J = 8.6 Hz, *meta* to −OCO−), 8.18 (d, 2ArH, J = 8.9 Hz, *meta* to −COO−).

10-(4-(4′-(4″-(2-Fluorooctyloxy)phenylcarbonyloxy))-biphenoxy)decyl (2,5-Bromo-3-thienyl)acetate (M2). Compound **7 (**1.36 g, 2.3 mmol) was added to a mixture of **9** (1.02 g, 3.4 mmol), DMAP (145 mg, 3.4 mmol), and DCC (702 mg, 3.4 mmol) in 50 mL of absolute $\mathrm{CH_2Cl_2}$, and the solution was stirred for 24 h at room temperature under an argon atmosphere, TLC indicated completion of the reaction. Then the solution was filtered to remove the urea crystals, and the solvent was removed under reduced pressure. The crude product was purified by column chromatography (*n*-hexane/ethyl acetate = 2/1) and recrystallized from a *n*-hexane:ethanol mixture (=9/1) to give 1.70 g of **M2** as colorless crystal in 85.0% yield. IR ($\mathrm{cm^{-1}}$): 2924, 2854, 1731, 1608, 1497, 1254, 1207, 1168, 1078, 801, 763. ^{1}H NMR ($\mathrm{CDCl_3}$, δ from TMS, ppm): 0.91 (t, 3H, J = 6.9 Hz, $-\mathit{CH}_3$), 1.20−1.82 (m, 26H, $-\mathrm{OCH_2CHF}(\mathit{CH}_2)_5\mathrm{CH_3}$; $-\mathrm{OCH_2}(\mathit{CH}_2)_8\mathrm{CH_2O}-$), 3.56 (s, 2H, $-\mathrm{C}\mathit{CH}_2\mathrm{COO}-$), 4.00 (t, 2H, J = 6.5 Hz, $-\mathrm{PhO}\mathit{CH}_2\mathrm{CH_2}-$), 4.11−4.22 (m, 2H, $-\mathrm{COO}\mathit{CH}_2\mathrm{CH_2}-$; $-\mathrm{PhO}\mathit{CH}_2\mathrm{CHF}-$), 4.80−4.94 (dm, 1H, $-\mathrm{OCH_2}\mathit{CHF}-$), 6.94 (s, 1ArH, $-\mathrm{SBrC}\mathit{CH}\mathrm{C}-$), 6.97 (d, 2ArH. J = 8.8 Hz, *ortho* to $-\mathrm{OCH_2CH_2}-$), 7.01 (d, 2ArH, J = 8.9 Hz, *ortho* to $-\mathrm{OCH_2CHF}-$), 7.24 (d, 2ArH, J = 8.6 Hz, *ortho* to −OCO−), 7.51 (d, 2ArH, J = 8.7 Hz, *meta* to $-\mathrm{OCH_2CH_2}-$), 7.58 (d, 2ArH, J = 8.6 Hz, *meta* to −OCO−), 8.18 (d, 2ArH, J = 8.9 Hz, *meta* to −COO−).

Scheme 2

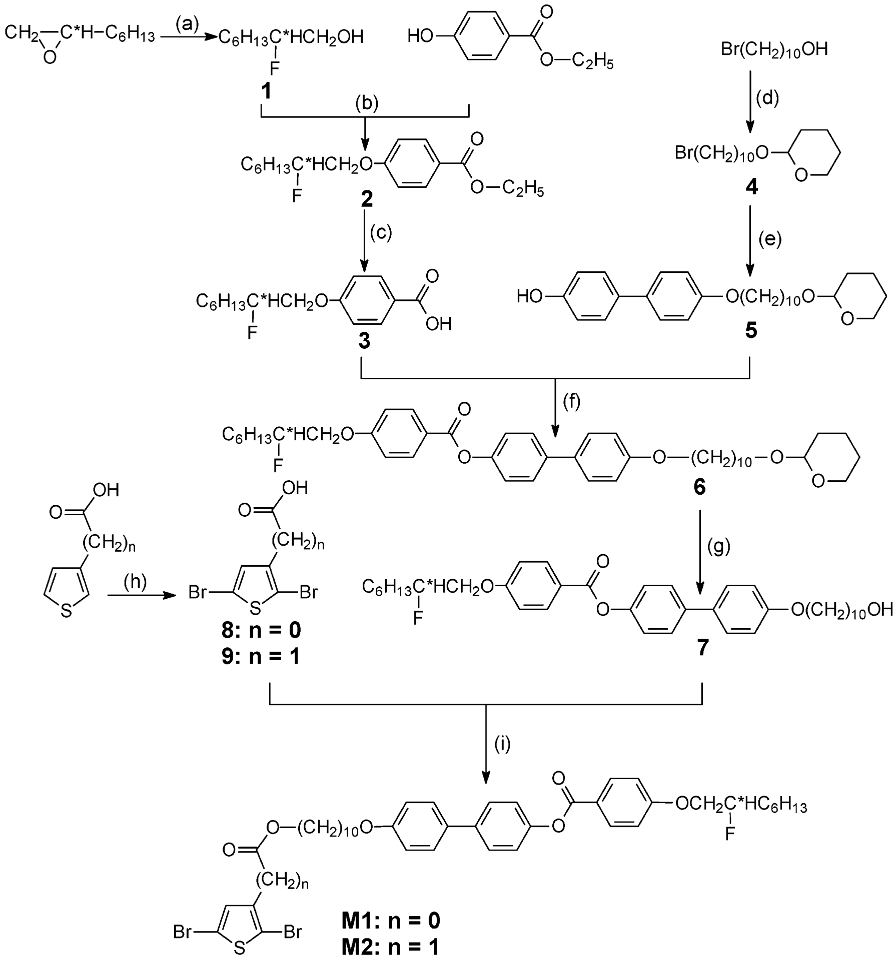

(a) pyridinium *poly*(hydrogen fluoride); (b) diethyl azodicarboxylate (DEAD), triphenylphosphine (TPP), THF; (c) KOH, CH_3OH, HCl; (d) 3, 4-dyhydro-2*H*-pyrane (DHP), pyridinium *p*-toluenesulfonate (PPTS), CH_2Cl_2; (e) 4,4'-biphenyldiol, K_2CO_3, *n*-butanol; (f), (i) *N,N'*-dicyclohexylcarbodiimide (DCC), 4-(dimethylamino)-pyridine (DMAP), CH_2Cl_2; (g) PPTS, C_2H_5OH; (h) *N*-bromosuccinimide, DMF.

3-(10-(4-(4′-(2-Fluorooctyloxy))biphenyloxy)decyloxycarbonloxy)methyl)-2,5-bromothiophene (M3). A mixture of compound **9** (508 mg, 1.69 mmol), DMAP (208 mg, 1.7 mmol), and DCC (351 mg, 1.7 mmol) in 25 mL of CH_2Cl_2 was stirred. Then compound **11** (400 mg, 0.85 mmol) in 10 mL of CH_2Cl_2 was added dropwise to the reaction mixture by a pressure-equalized dropping funnel and heated under reflux for 24 h under an argon atmosphere, TLC indicated completion of the reaction. The solution was filtered to remove the urea crystals, and the solvent in the filtrate was removed by evaporation. Purification by column chromatography (*n*-hexane/ethyl acetate = 9/1) afforded 0.561 g of **M3** in 87.5% yield. IR (cm^{-1}): 2920, 2854, 1739, 1608, 1502, 1276, 1252, 1178, 1044, 824, 808. ^{1}H NMR ($CDCl_3$, δ from TMS, ppm): 0.90 (t, 3H, J = 6.9 Hz, $-CH_3$), 1.19−1.86 (m, 26H, $-OCH_2(CH_2)_8CH_2O-$; $-CH_2CHF(CH_2)_5CH_3$), 3.56 (s, 2H, $-CCH_2COO-$), 3.99 (t, 2H, J = 6.5 Hz, $-PhOCH_2CH_2-$), 4.04−4.16 (m, 2H, $-PhOCH_2CHF-$), 4.11 (t, 2H, J = 6.7 Hz, $-COOCH_2CH_2-$), 4.77−4.91 (dm, 1H, $-OCH_2CHF-$), 6.93 (s, 1ArH, $BrCCHC-$), 6.94−6.96 (dd, 4ArH, J = 8.7 Hz, *ortho* to $-OCH_2CHF-$, *ortho* to-OCH_2CH_2-), 7.46−7.47 (dd, 4ArH, J = 8.6 Hz, *meta* to $-OCH_2CHF$-, *meta* to $-OCH_2CH_2-$).

Poly[10-(4-(4′-(4″-(2-fluorooctyloxy)phenylcarbonyloxy))biphenoxy)decyl-thiophene-3-carboxylate] (P1). In a Schlenk flask, a mixture of DMF (4 mL) and 2,2′-bipyridine, bpy (0.14 g, 0.9 mmol), and Ni(COD)$_2$ (COD = cyclooctadiene) (0.25 g, 0.9 mmol) was stirred under an argon atmosphere. The color of the solution changed from yellow to green to purple, which was consistent with the formation of Ni(COD)(bpy) in the solution. Then **M1** (0.61 g, 0.7 mmol) in 2 mL of DMF was added to the catalyst solution. The solution was heated under reflux at 100 °C for a further 5 days. Then the flask was allowed to cool to room temperature. The reaction mixture was poured into a large amount of methanol (500 mL) and vigorously stirred for 24 h. The resulting precipitate was collected by filtration and dissolved in minimum amount of THF and stirred in methanol containing HCl for 24 h. After filtration, the product was dried under vacuum to give 480 mg as brown powder in 96.4% yield. IR (cm^{-1}): 2927, 2854, 1718, 1606, 1497, 1253, 1207, 1166, 1073, 763. ^{1}H NMR ($CDCl_3$, δ from TMS, ppm): 0.90 (br, 3H, $-CH_3$), 1.19−1.86 (m, 26H, $-OCH_2CHF(CH_2)_5CH_3$; $-OCH_2(CH_2)_8CH_2O-$), 3.92 (m, 2H, $-PhOCH_2CH_2-$), 4.13 (m, 2H, $-PhOCH_2CHF-$), 4.28 (m, 2H, $-COOCH_2CH_2-$), 4.79−4.88 (dm, 1H, $-OCH_2CHF-$), 6.90−6.98 (dm, 4ArH, 2H, *ortho* to $-OCH_2CH_2-$; 2H, *ortho* to $-OCH_2CHF-$), 7.21 (dm, 2ArH, *ortho* to $-OCO-$), 7.34−7.53 (m, 5ArH, 1H, $-SCCHC-$; 2H, *meta* to $-OCH_2CH_2-$; 2H, *meta* to $-OCO-$), 8.14 (m, 2ArH, *meta* to $-COO-$).

Poly[10-(4-(4′-(4″-(2-fluorooctyloxy)phenylcarbonyloxy))biphenoxy)decyl-3-thienyacetate] (P2). P2 was prepared using a method similar to that described for **P1**. Quantities used: bpy (160 mg, 1.0 mmol) and Ni(COD)$_2$ (280 mg, 1.0 mmol) in DMF (8 mL) and **M2** (0.70 g, 0.8 mmol) in DMF (4 mL). Yield: 516 mg, 89.4%. IR (cm^{-1}): 2928, 2854, 1723, 1605, 1498, 1252, 1205, 1202, 1074, 802, 763. ^{1}H NMR ($CDCl_3$, δ from TMS, ppm): 0.89 (m, 3H, $-CH_3$), 1.21−1.74

Scheme 3

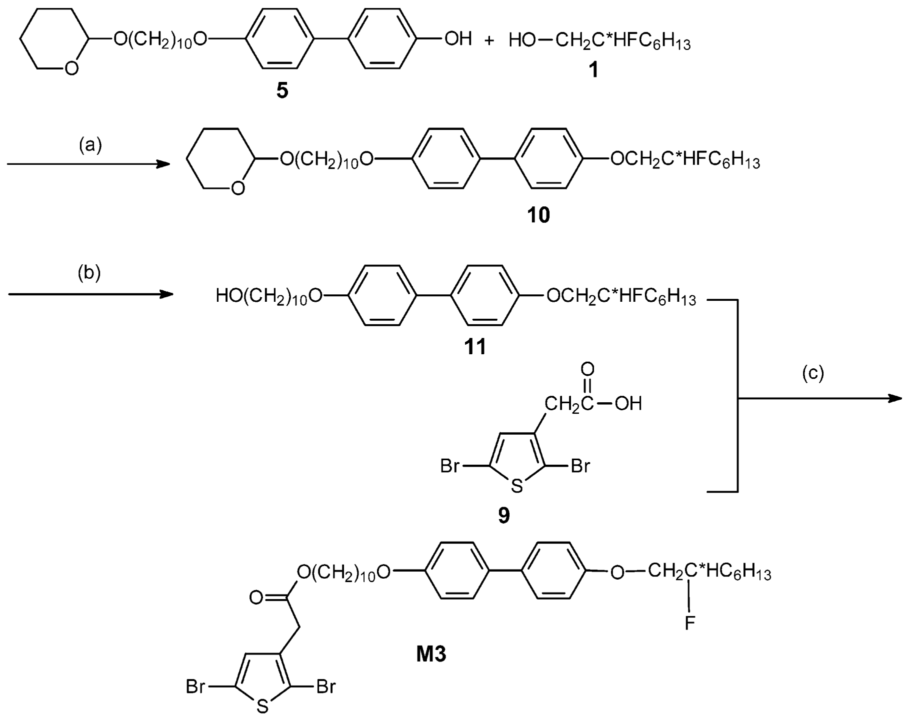

(a) DEAD, TPP, THF; (b) PPTS, C_2H_5OH; (c) DCC, DMAP, CH_2Cl_2

(m, 26H, $-OCH_2CHF(CH_2)_5CH_3$; $-OCH_2(CH_2)_8CH_2O-$), 3.56 (m, 2H, $-CCH_2COO-$), 3.93 (m, 2H, $-PhOCH_2CH_2-$), 4.08−4.13 (m, 4H, $-COOCH_2CH_2-$; $-PhOCH_2CHF-$), 4.79−4.88 (dm, 1H, $-OCH_2CHF-$), 6.91 (d, 2ArH, $J = 7.6$ Hz, *ortho* to $-OCH_2CH_2-$), 6.97 (d, 2ArH, $J = 8.3$ Hz, *ortho* to $-OCH_2\text{-}CHF-$), 7.12 (m, 1ArH, $-SCCHC-$), 7.20 (d, 2ArH, $J = 7.8$ Hz, *ortho* to $-OCO-$), 7.45 (d, 2ArH, $J = 8.0$ Hz, *meta* to $-OCH_2CH_2-$), 7.53 (d, 2ArH, $J = 7.6$ Hz, *meta* to $-OCO-$), 8.13 (d, 2ArH, $J = 7.9$ Hz, *meta* to $-COO-$).

3-(10-(4-(4′-(2-Fluorooctyloxy))biphenyloxy)decyloxycarbonloxy)methyl)-2,5-bromothiophene (P3). **P3** was prepared using a method similar to that described for **P1**. Quantities used: bpy (137 mg, 0.88 mmol) and $Ni(COD)_2$ (243 mg, 0.88 mmol) in DMF (7 mL) and **M3** (0.50 g, 0.7 mmol) in DMF (4 mL). Yield: 337 mg, 67.5%. IR (cm^{-1}): 2927, 2854, 1737, 1608, 1500, 1469, 1247, 1176, 823. ^1H NMR ($CDCl_3$, δ from TMS, ppm): 0.83 (t, 3H, $J = 6.5$ Hz, $-CH_3$), 1.18−1.73 (m, 26H, $-OCH_2(CH_2)_8CH_2O-$, $-CH_2CHF(CH_2)_5CH_3$), 3.51 (m, 2H, $-CCH_2COO-$), 3.85−3.92 (m, 2H, $-PhOCH_2CH_2-$), 3.99−4.06 (m, 4H, $-PhOCH_2CHF-$, $-COOCH_2CH_2-$), 4.71−4.81 (dm, 1H, $-OCH_2CHF-$), 6.85−6.93 (m, 4ArH, 2H, *ortho* to $-OCH_2CH_2-$; 2H, *ortho* to $-OCH_2CHF-$), 7.37−7.39 (m, 5ArH, 1H, $-SCCHC-$, 2H, *meta* to $-OCH_2CH_2-$; 2H, *meta* to $-OCH_2CHF-$).

3. Results and Discussion

The synthetic routes of the monomers and polymers are shown in Scheme 2. The chiral alcohol (*S*)-2-fluorooctanol (**1**) was prepared according to the method suggested by Nohira et al.,[23] in which (*R*)-(+)-1,2-epoxyoctane was reacted with pyridinium poly(hydrogen fluoride) in ether.

In Scheme 2, ethyl 4-[(*S*)-2-fluorooctoxy]benzoate (**2**) was synthesized by coupling **1** with ethyl *p*-hydroxybenzoate via Mitsunobu reaction in THF.[24] The basic hydrolysis of **2** with KOH in a solution of methanol and water gave 4-[(*S*)-2-fluorooctoxy]benzonic acid (**3**).

The hydroxyl group of 10-bromodecanol was protected as a tetrahydropyranyl ether (**4**). Compound **5** was prepared by reacting **4** with 4,4′-dihydroxybiphenyl in the presence of K_2CO_3. The esterification between **5** and **3** in the presence of dicyclohexylcarbodiimide (DCC) and 4-(dimethylamino)pyridine (DMAP) gave compound **6**. Deprotection of **6** was carried out in the presence of pyridinium *p*-toluenesulfonate (PPTS), giving compound **7**.

Bromination of thiophene-3-carboxylic acid and 2-(3-thienyl)acetic acid with *N*-bromosuccinimide (NBS) in DMF resulted in the formation of 2,5-dibromothiophene-3-carboxylic acid (**8**) and 2,5-dibromothiophene-3-acetic acid (**9**). The 2,5-dibrominated thiophene monomers, **M1** and **M2,** were synthesized by esterification between **7** and **8**, and **7** and **9**, respectively, under the same conditions as that of the synthesis of **6**.

The other type of thiophene monomer, **M3**, was synthesized as in Scheme 2, but two aromatic rings were employed in the mesogenic core.

The LC groups of **M1** and **M2** are composed of a biphenyl moiety linked with a phenyl moiety via an ester linkage as a mesogenic core, a decamethylene chain as a spacer, and a (*S*)-2-fluorooctyloxy group as a terminal moiety. Meanwhile, the LC group of **M3** is composed of a biphenyl moiety as a mesogenic core, a decamethylene chain as a spacer, and a (*S*)-2-fluorooctyloxy group as a terminal moiety. The polymerizations of 2,5-dibrominated thiophene monomers were carried out via dehalogenative polycondensation, giving poly(3-FLC substituted thiophene) derivatives, **P1**, **P2**, and **P3**.

All polymers synthesized (**P1**, **P2**, and **P3**) were fusible and soluble in common organic solvents including tetrahydrofuran (THF). Number-average (M_n) and weight-average (M_w) molecular weights of **P1**, **P2**, and **P3** are summarized in Table 1. M_n range from 4800 to 12 000, and M_w range from 12 800 to 54 800. The chemical structures of the polymers were confirmed by ^1H NMR. ^{19}F NMR of **P2** in $CDCl_3$ showed a peak at $\delta = -186.39$, which is assignable to a fluorine atom attached to the chiral center ($CF_3C_6H_5$ as a standard,

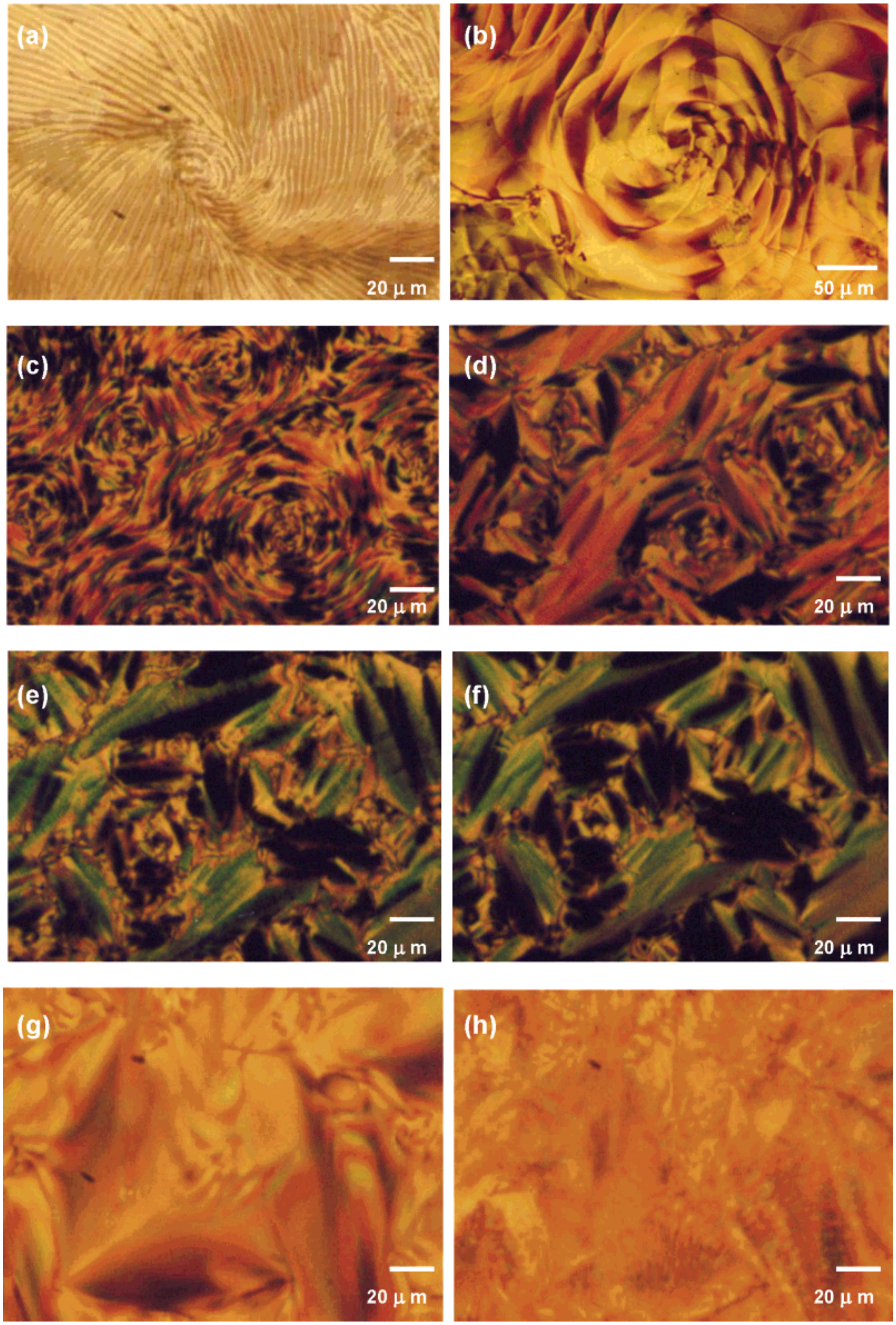

Figure 1. (a, b) Polarizing optical micrographs of compound **6**; (a) "shell"-printed texture of SmC* phase at 104 °C, (b) striated "rose" texture of SmI* phase at 91 °C. (c, d) **M1**; (c) filament texture of TGBA* at 131 °C; (d) "rose" texture of SmA* phase at 120 °C. (e, f) **M1**; (e) striated "rose" texture of SmC* phase at 85 °C, (f) "rose" texture of SmB* phase at 83 °C. (g, h) **P2**; (g) fan-shaped texture of SmA* phase at 194 °C; (h) striated fan-shaped texture of SmC* phase at 144 °C.

$\delta_{\text{standard}} = 63.72$ ppm). The polarizing optical micrographs of **6**, **M1**, and **P2** are shown in Figure 1.

In the case of compound **6**, upon cooling from the melting point of 151 °C, a N* phase with fingerprint texture[26−28] was observed at 149 °C, the texture changed into a "shell"-printed texture of chiral smectic C (SmC*) phase at 139 °C, and striated "rose" texture of chiral smectic I (SmI*) phase[29,30] appeared at 96 °C. Finally, compound **6** changed into crystal at 77 °C via the SmJ* phase. Also, compound **7** shows SmC*. **M1** showed a

Table 1. Polymerization Results

polymer	M_n	M_w	MWD	DP[a]
P1	12 000	47 400	3.9	17
P2	11 600	54 800	4.7	16
P3	4 800	12 800	2.6	8

[a] DP (degree of polymerization) = M_n/mru (mru: mass of monomer repeat unit).

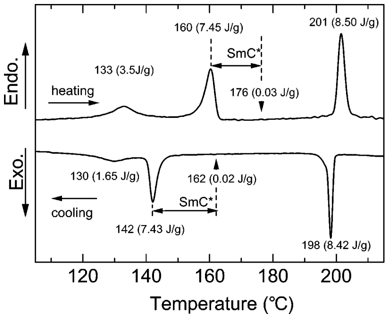

Figure 2. DSC curves of **P2**.

Table 2. Phase Transition Temperatures of LC Precursor, Monomers, and Polymers[a]

Compd	Phase transition temperatures (°C)	
	Heating	Cooling
3	C 105 SmX 121 N* 138 Iso*	C 96 SmX 118 N* 135 Iso*
6	C 89 SmX 98 SmC* 141 N* 151 Iso*	C 77 SmJ* 85 SmI* 96 SmC* 139 N* 149 Iso*
7	C 152 SmC* 159 N* 180 Iso*	C 136 SmC* 150 N* 176 Iso*
M1	C 79 SmB* 86 SmC* 102 SmA* 131 N* 139 Iso*	C 52 SmB* 84 SmC* 94 SmA* 130 TGBA* 131 N* 138 Iso*
M2	C 59 C$_1$ 71 SmX 92 SmC* 104 SmA* 128 N* 132 Iso*	C 50 SmX 90 SmC* 104 SmA*127 N* 131 Iso*
***P*1**	g 197 SmA *203 Iso*	g 147 SmA* 174 Iso*
***P*2**	g 133 SmB* 160 SmC* 176 SmA* 201 Iso*	g 130 SmB* 142 SmC* 162 SmA* 198 Iso*
***P*3**	g 95 SmA* 100 Iso*	g 92 SmX 96 SmA* 98 Iso*

[a] Iso* = isotoropic phase, N* = chiral nematic phase, SmA* = chiral smectic A, SmB* = chiral smectic B, SmC* = chiral smectic C, SmI* = chiral semctic I, SmJ* = chiral smectic J, TGBA* = twist grain boundary A, g = glassy state; C, C$_1$ = crystal, SmX = unidentified smectic phases.

twist grain boundary (TGBA*) phase[31] at 131 °C with a filament texture and SmC* at 94 °C in the cooling process. The stripes appeared in the fan-shaped texture in the SmC* as shown in Figure 1e. The stripes disappeared in the SmB* phase[32,33] at 83 °C (Figure 1f). **M2** showed SmC* phase between 104 and 90 °C in the cooling process. All polymers exhibited mesophases. **P1** showed enantiotropic SmA* phases; however, no SmC* phase corresponding to ferroelectric LC was exhibited. **P2** exhibited SmC* phase with a striated fan-shaped texture between 162 and 142 °C in the cooling process and between 160 and 176 °C in the heating process. DSC curves of **P2** are shown in Figure 2. The DSC show that the SmA* to SmC* transition was extremely weak due to second order in nature. However, the change of the optical texture at the transition temperature was clearly observed under POM observations. Phase transition temperatures are summarized in Table 2.

Generally, there are two possible structures for the LC-substituted polythiophene derivatives, where the side chains are located on either one side or both sides of the main chain in the LC layers. They are abbreviated as "one-sided" and "both-sided" structures, respectively. In the case of **P2**, MM calculations imply that the *d*-spaces (interlayer distance) of one-sided and both-sided structures of the layer length are 46.2 and 89.8 Å, respectively. The XRD pattern of **P2** measured in the LC phase at 180 °C showed two reflection peaks corresponding to distances of 4.60 and 37.6 Å. The *d*-space of 37.6 Å is closer to that suggested for one-sided structure. When the temperature was lowered to 160 °C, the *d*-spacing of the small-angle reflection decreased from 37.6 to 35.4 Å, suggesting the formation of a SmC* phase.[34] The striated fan-shaped texture of SmC* phase of **P2** was observed at this temperature (Figure 1h). When the temperature was further lowered to 135 °C, the *d*-spacing of the small angle reflection increased from 35.4 to 39.1 Å due to the tilted molecules aligning perpendicular to the layer with the phase transition from SmC* to SmB*. Another phase transition between SmB* and the glassy state is possible because the XRD pattern of SmB* at the wide-angle region becomes sharp at room temperature. However, the optical texture of the polymer showed no change at room temperature, and DSC showed no peak for the

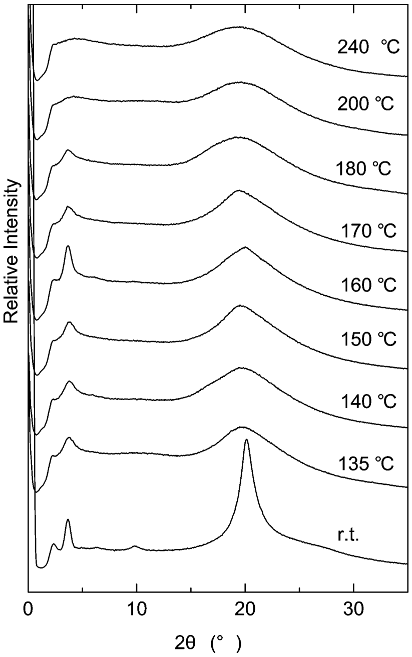

Figure 3. XRD profile of **P2**.

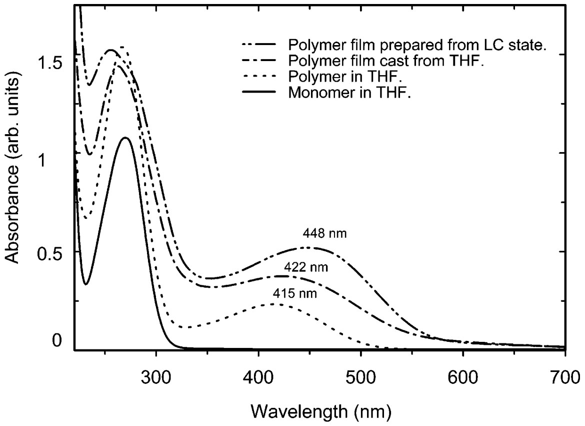

Figure 4. UV–vis absorption spectra of **M1** and **P1** film and solution in THF.

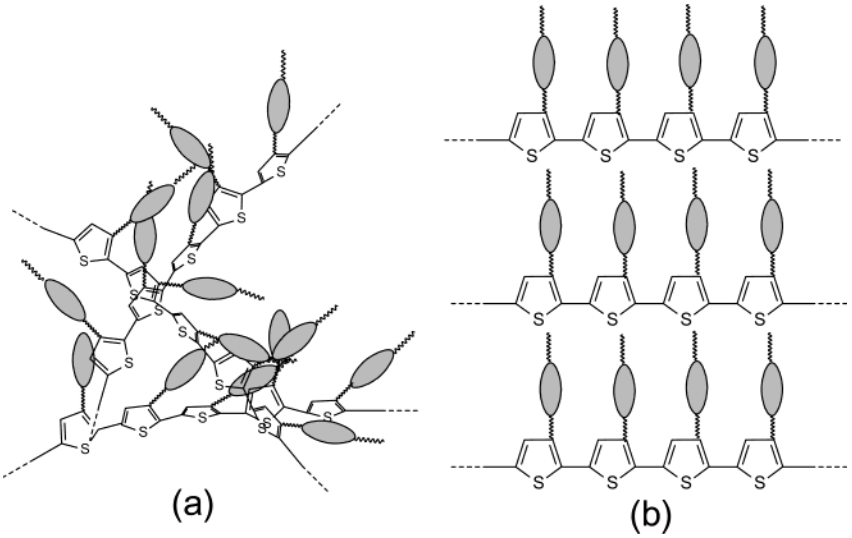

Figure 5. Possible structures of the LC polymer: (a) polymer in solution, isotropic, or solid state after removal of the solvent; (b) in the LC state.

Table 3. Absorption Maximum Values of the Polymers

polymer	λ_{max} (nm), $\pi \rightarrow \pi^*$ transition of polymer main chain in THF (nm)	 cast film (nm)	 film prepared from LC state (nm)
P1	415	422	448
P2	400	409	424
P3	340	*a*	*a*

[a] No self-standing film was obtained.

SmB*−glassy transition below 130 °C. This is the first observation of a SmC* phase in LC polythiophene derivatives, which allows us to predict the evolution of ferroelectricity in this polymer. On the other hand, **P3** showed SmA* and SmX phases on the cooling process. XRD analysis suggested that **P3** may have a higher order smectic phase. The XRD profile of **P2** is shown in Figure 3.

UV−vis absorption spectra of **P1** as well as the corresponding monomer (**M1**) are shown in Figure 4. The two absorption bands at 267 and 415 nm observed for a THF solution of **P1** are assigned to the $\pi-\pi^*$ transition of the mesogenic core of the side chain and that of the conjugated main chain, respectively. In fact, **M1** only showed an absorption band at 265 nm, which is assigned to the $\pi-\pi^*$ transition of the mesogenic substituent. The absorption band due to the conjugated main chain of **P1** was slightly red-shifted to 422 nm in the case of a cast film. This may be due to the fact that the in-plane alignment occurred in the cast film.

It is of interest to note that a remarkable red shift to 448 nm was observed when the cast film was heated to the isotropic phase and then cooled through the LC state to the solid state. This shift can be rationalized with the enhancement of π-conjugation of the main chain. In the LC phase, the LC side chains spontaneously orient themselves in such a way that alignment of the main chain should give rise to increase of the coplanarity of the conjugated main chain (Figure 5). The same red shift was also observed in **P2**. Absorption maxima of the polymers are summarized in Table 3.

The temperature dependence of the dielectric constant of **P2** is shown in Figure 6. It was observed that the dielectric constant increased sharply in the temperature range of SmC* phase. This behavior is typical of FLCs. At the same time, the dielectric constant of the polymer increased with decreasing frequency.

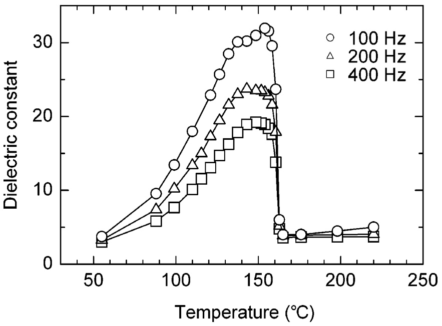

Figure 6. Temperature dependence of dielectric constant of **P2**.

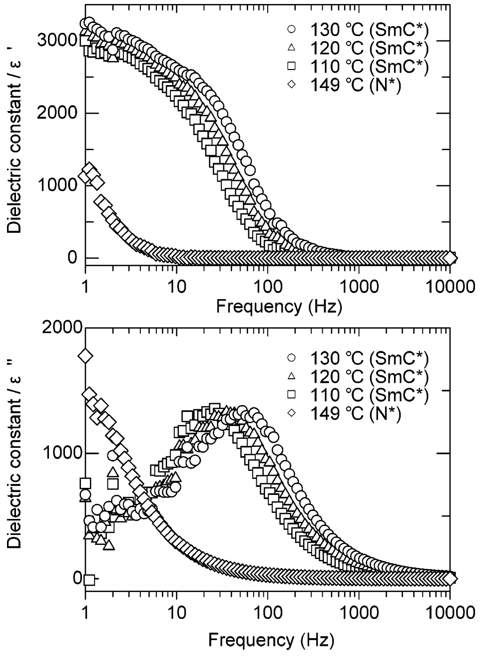

Figure 7. Dielectric constant of compound **6** as a function of frequency.

A discussion of relaxation times, relaxation strength, and the origin of a relaxation process is possible using a frequency dependence measurement of the dielectric real part (ϵ') and imaginary part (ϵ''). ϵ' and ϵ'' are

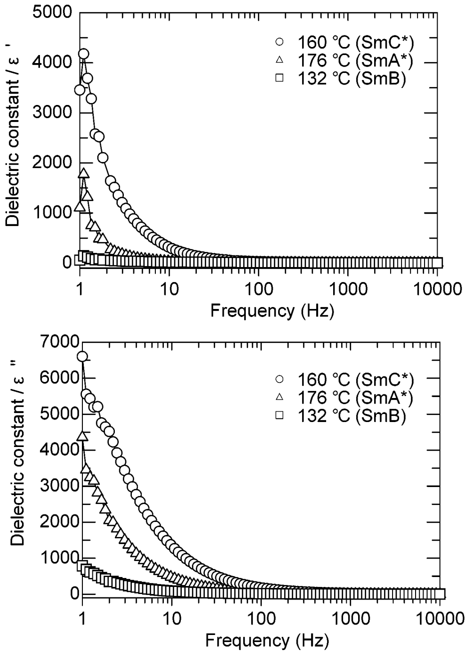

Figure 8. Dielectric constant of **P2** as a function of frequency.

estimated by the following equations

$$\epsilon' = C_s/C_0$$

$$\epsilon'' = 1/\omega R_s C_0$$

where C_s is the capacitance of sample, C_0 is the capacitance of cell (vacuum capacitance), ω is the angular frequency, and R_s is the resistance of the sample.

Relaxation time varies relative to the molecular orientation process. The frequency at a point of inflection in the real part corresponds to the frequency at a maximum peak in the imaginary part, and the response time can be obtained from the inverse of the frequency. The frequency dependence of dielectric measurements was carried out for compounds **6** and **P2**.

Dielectric constants of the real part and imaginary part as a function of frequency for **6** in the SmC* and N* phases at corresponding temperatures are shown in Figure 7.

In the S_C* phase at 130 °C, a point of inflection and a maximum are observed at ~100 Hz in both the dielectric real part and imaginary part. Therefore, the response time of **6** in the SmC* phase at 130 °C is ~10^{-2} s. Response times became slower in lower temperatures in the SmC* phase because viscosity increased with decreasing temperature. Also, the LC polymer would have a higher elastic constant and twist viscosity,[35] which should cause a reduction in response time.

The response time of **6** in N* phase was ~1 s. The response time in the SmC* phase was faster and dielectric constants in the SmC* phase are larger than in the N* phase for **6**. These tendencies are typical of FLC according to the ferroelectric Goldstone mode.

Dielectric constants of **P2** as a function of frequency are shown in Figure 8. The response time of the SmC* phase at 160 °C is ~1 s estimated by ϵ' maximum at 1.1 Hz and ϵ'' inflection at 1.5 Hz. The response time of **P2** with respect to external electric fields was slower than that of compound **6** in the SmC* phase. Molecular rotation of the polymer side chains can be restricted by the main chain, but **6**, as a low molecular weight FLC, is free from such a restriction. In other words, the polymer main chain moves with the FLC side chains.

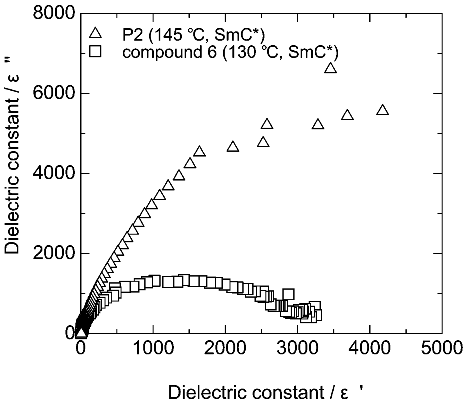

Figure 9. Cole−Cole diagram of compounds **6** and **P2**.

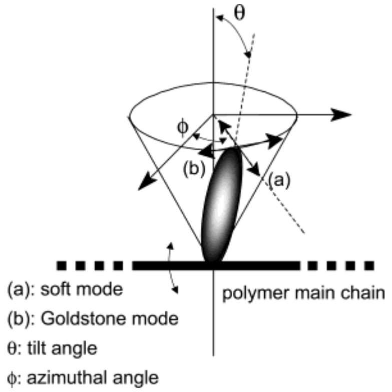

Figure 10. Molecular relaxation modes of FLC polymer.

Cole−Cole diagrams of compounds **6** and **P2** are shown in Figure 9. Here, the radius of the Cole−Cole plot is equal to $\Delta\epsilon/2$, where $\Delta\epsilon$ is relaxation strength. The relaxation strength of compound **6** was 3000. Although **P2** shows no complete semicircle in the Cole−Cole plot, the relaxation strength of **P2** could be greater than that of **6**. The possible modes of the polymer are shown in Figure 10.FLC molecules strongly depend on the ferroelectric Goldstone mode, but in the case of FLC polymers, the modes include not only the Goldstone mode of side chains but also a mode representing the molecular movement of the main chain with respect to the rotation of the side chain. Furthermore, orientation of the polymer main chain with respect to the electric field may be considerable. The FLC conjugated polymers may have several relaxation modes.

It is possible to assume that the LC side chains align themselves with polymer main chain, and this order allows a regulated SmC* array. This order may provide higher relaxation strength. This could be referred to as polymer effects.

However, we need to take into account that the larger relaxation strength value of **P2** may be the result of an ionic impurity.

We carried out measurements of optical response time. The optical response time of **P2** was ~1 s with the application of DC 2 kV/cm to a **P2** sandwiched ITO glass cell at 150 °C. This value is consistent with the value obtained through measurements of dielectric constant.

Conclusion

Novel LC polythiophene derivatives were synthesized by introducing a fluorine-containing chiral LC group onto the side chains. One of the polymers (**P2**) showed SmC* phase with an enantiotropic behavior, whose LC temperature range was as wide as 20 deg. This is the first reported case of a SmC* phase being observed in a polythiophene derivative. It is therefore expected that these polymers should be usable as ferroelectric LC conducting materials. It was also found that the effective conjugation length of the main chain increased after the spontaneous orientation of the LC side chains. The ferroelectric behavior was confirmed by examining thetemperature dependence of the dielectric constant of the polymer.

Acknowledgment. We are grateful to Dr. Hiroshi Yokoyama (National Institute of Advanced Industrial Science and Technology, AIST) for his help in the measurement of the dielectric constants of the polymers. We thank Prof. Hideki Shirakawa for valuable discussions and advice. The authors also acknowledge Messrs. Stephan Bell and Takenori Ueoka (University of Tsukuba) for their kind assistance. This work was supported by Grant-in-Aids for Scientific Research from the Ministry of Education, Culture, Sports, Science and Technology, Japan, and "Promotion of Creative Interdisciplinary of Materials Science for Novel Functions" of the 21st century Center of Excellence (COE) program of the Ministry of Education, Culture, Sports, Science and Technology, Japan.

References and Notes

(1) Oh, S.-Y.; Akagi, K.; Shirakawa, H.; Araya, K. *Macromolecules* **1993**, *26*, 6203.
(2) Akagi, K.; Goto, H.; Kadokura, Y.; Shirakawa, H.; Oh, S.-Y.; Araya, K. *Synth. Met.* **1995**, *69*, 13.
(3) Akagi, K.; Shirakawa, H. *Macromol. Symp.* **1996**, *104*, 137.
(4) Akagi, K.; Shirakawa, H. *The Polymeric Materials Encyclopedia. Synthesis, Properties and Applications;* CRC Press: Boca Raton, FL, 1996; Vol. 5, p 3669.
(5) Akagi, K.; Shirakawa, H. In Wise, D. L., et al., Eds. *Electrical and Optical Polymer Systems: Fundamentals, Methods, and Applications;* Marcel Dekker: New York, 1998; Vol. 28, p 983.
(6) Dai, X. M.; Goto, H.; Akagi, K.; Shirakawa, H. *Synth. Met.* **1999**, *102*, 1289.
(7) Dai, X. M.; Goto, H.; Akagi, K.; Shirakawa, H. *Synth. Met.* **1999**, *102*, 1291.
(8) Hong, X.-M.; Cameron T, J.; Collard, D. *Macromolecules* **2000**, *33*, 3502.
(9) Hong, X.-M.; Collard, D. *Macromolecules* **2000**, *33*, 6916.
(10) Schartel, B.; Wachtendorf, V.; Grell, M.; Bradley, D. D.C.; Hennecke, M. *Phys. Rev. B: Condens. Matter Mater. Phys.* **1999**, *60*, 277.
(11) Park, J. H.; Lee, C. H.; Akagi, K.; Shirakawa, H.; Park, Y. W. *Synth. Met.* **2001**, *119*, 633.
(12) Pei, J.; Yu, W.-L.; Ni, J.; Lai, Y.-H.; Huang, W.; Heeger, A. J. *Macromolecules* **2001**, *34*, 7241.
(13) Grell, M.; Bradley, D. D. C.; Long, X.; Chamberlain, T.; Inbasekaran, M.; Woo, E. P.; Soliman, M. *Acta Polym.* **1998**, *49*, 439.
(14) Neher, D. *Macromol. Rapid Commun.* **2001**, *22*, 1365.
(15) Osaka, I.; Goto, H.; Itoh, K.; Akagi, K. *Synth. Met.* **2001**, *119*, 541.
(16) Oguma, J.; Kawamoto, R.; Goto, H.; Itoh, K.; Akagi, K. *Synth. Met.* **2001**, *119*, 537.
(17) Oda, M.; Nothofer, H.-G.; Lieser, G.; Scherf, U.; Meskers, S. C. J.; Neher, D. *Adv. Mater.* **2000**, *12*, 362.
(18) Dai, X. M.; Goto, H.; Akagi, K.; Shirakawa, H. *Kobunshi Ronbunshu* **1999**, *56*, 797.
(19) Mitsuishi, M.; Ito, S.; Yamamoto, M.; Endo, H.; Hachiya, S.; Fischer, T.; Knoll, W. *Macromolecules* **1998**, *31*, 1565.
(20) Hwang, J.-C.; Fuwa, Y.; Moritake, H.; Gu, H.; Ozaki, M.; Yoshino, K. *Jpn. J. Appl. Phys., Part 2: Lett.* **1995**, *34*, L560.
(21) Leister, N.; Geschke, D. *Liq. Cryst.* **1998**, *24*, 441.
(22) Fukuda, A.; Takanishi, Y.; Isozaki, T.; Ishikawa, K.; Takezoe, *J. Mater. Chem.* **1994**, *4*, 997.
(23) Nohira, H.; Nagamura, S.; Kamei, M. *Mol. Cryst. Liq. Cryst.* **1990**, *180B*, 379.
(24) Mitsunobu, O.; Yamada, M. *Bull. Chem. Soc. Jpn.* **1967**, *40*, 2380.
(25) Akagi, K.; Goto, H.; Shirakawa, H. *Synth. Met.* **1997**, *84*, 313.
(26) Scheffer, T. J.; Gruler, H.: Meier, G. *Solid State Commun.* **1972**, *11*, 253.
(27) Meyer, R. B.; Pershan, P. S. **1973**, *3*, 989.
(28) Arora, S. L.; Fergason, J. L.; Saupe, A. *Mol. Cryst. Liq. Cryst.* **1970**, *10*, 243.
(29) Richter, L.; Demus, D.; Sackmann, H. **1981**, *71*, 269.
(30) Gane, P. A. C.; Leadbetter, A. J.; Wrighton, P. G. **1981**, *66*, 247.
(31) Dierking, I.; Lagerwall, T. *Liq. Cryst.* **1999**, *26*, 83.
(32) Sackmann, H.; Demus, D. *Mol. Cryst. Liq. Cryst.* **1966**, *2*, 81.
(33) Leadbetter, A. J.; Frost, J. C.; Mazid, M. A. *J. Phys., Lett.* **1979**, *40*, 325.
(34) de Vries, A. *Mol. Cryst. Liq. Cryst.* **1985**, *131*, 135.
(35) Legrand, C.; Parneix, J. P. *J. Phys.* (*Paris*) **1990**, *51*, 787.

MA0354492